

Jacobians of ECMWF Prognostic and Diagnostic Cloud Schemes

Luc Fillion¹ and Jean-François Mahfouf²

¹*Direction de la Recherche en Météorologie, Meteorological Service of Canada*

²*European Centre for Medium-Range Weather Forecast, Reading, England*

Abstract

A detailed examination of the sensitivity properties of Tiedtke's prognostic cloud scheme operational at the European Center for Medium-Range Weather Forecasts (ECMWF) is done. The coupling of the cloud scheme with the ECMWF convective mass-flux scheme is considered. The sensitivity of the scheme is split into all its contributing parts in order to extract the dominant terms. A wide variety of convective cases normally present in a regular operational forecast is considered. Some comparisons are made with two other types of diagnostic cloud schemes.

It is shown that the main contributing terms to the liquid-water/ice (LWI) sensitivity are (1) for deep convective cases (tropics and extra-tropics): detrainment terms from moist convection, evaporation processes and conversion of cloud water into rain. The structure of the jacobian in terms of temperature and moisture perturbations in such cases being strongly dominated by the structure of the jacobian of the convective mass flux. Jacobians from the diagnostic cloud scheme being significantly different from the jacobian of the prognostic cloud scheme except for the total liquid-water/ice jacobians where some similarities exist, (2) for shallow convection cases: The same terms as for deep convective cases are important (convective effects still dominate) but now, erosion of clouds becomes important (least important term however). Total LWI jacobians for diagnostic and prognostic cloud schemes here also are similar, still because of dominance of convective effects, although jacobians of LWI are significantly different. When moist-convection plays a negligible role (e.g. as in convection called mid-level convection in Tiedtke's operational convective scheme), the dominant terms are erosion of clouds, condensation/evaporation effects and conversion of cloud water into rain.

1. Introduction

A major challenge currently facing operational centers performing variational data assimilation is the incorporation of satellite information over cloudy regions. For instance, from these radiance measurements, it is possible to relate them with the atmospheric total liquid-water/ice content, specific humidity and temperature using radiative transfer models. Although this relationship can readily be established in the context of model cloud processes, their use in a variational assimilation context represents a major challenge. This is due to the level of error in such physical parameterizations in addition to their strong variability in space and time. Assuming suitable error characterization can be achieved (an aspect not considered here) there remains the non-negligible task of demonstrating the usefulness of linearized versions of these processes. This is a crucial aspect that needs clarification prior to their use in a variational data assimilation context, more precisely the tangent-linear versions of the nonlinear code must prove robust and accurate.

Corresponding author address: Dr. Luc Fillion, Direction de la Recherche en Météorologie, Meteorological Service of Canada, 2121 Route Transcanadienne, Dorval, Qc, Can, H9P 1J3

The importance of each term appearing in Eq. (2.1) below on the hydrological cycle has been described in Tiedtke (1993, see their Figure 8) (hereafter referred to as T93). The design and tuning of such schemes is an important step before operational implementation and its impact on forecast has been carefully examined. In the context of variational data assimilation however, the problem can be quite different. The first requirement is the construction of the tangent-linear version of the scheme even-though the tangent-linear (TL) scheme could be avoided (using two nonlinear run) but is required for the adjoint (ADJ) operators. Details of such requirements in particular for the assimilation of cloud properties can be found in Janiskova et al. 2000. This refers to the differentiability of the nonlinear scheme. Because of the nature of the physical problem, the introduction of conditionals on the thermodynamical properties of the atmospheric state must be carefully monitored while computing each term in the equations. A simple example of this is the conditional on supersaturation. Unfortunately, this introduces functional discontinuities which directly impacts the differentiability condition. More extensive use of a statistical approaches to cloud process parameterization (e.g. Thompkins 2002) can in principle alleviate such loss of differentiability. It is clear at this stage that straightforward linearization of the full scheme (with ad-hoc assumptions at points of discontinuity) and direct use in a variational assimilation context (including the adjoint scheme) can generate erroneous results. An important question is then to focus attention to those terms which are dominant in the perturbation equation. If discontinuities appear in terms of the basic equations having negligible contributions to the perturbation of the total tendencies, the simple remedy is to just ignore these terms. It is worth noting that this systematic examination has already been adopted in the perturbation model approach (including dynamical processes) for variational data assimilation at the Met Office. This systematic examination of dominant terms is not only useful to limit impacts of discontinuities, but is also extremely important to understand when important nonlinearities also impact the degree of validity of the tangent-linear approximation of the scheme.

This study is a first attempt in this direction. The major motivation came from the need to gain understanding on the sensitivity of the cloud parameterization at ECMWF in order to design satellite cloud data assimilation strategies. Because this cloud parameterization scheme has two prognostic variables, it raises the issue of an appropriate definition of control variables to assimilate such cloud data. Therefore alternative approaches provided by diagnostic cloud schemes are also considered here. The experiments considered here were designed basically to clarify these various aspects. Section 2 describes the model and cloud schemes considered. Section 3 gives the details of the experiments performed and section 4 gives the results obtained. A summary and useful conclusions are presented in section 5.

2. Prognostic and diagnostic cloud schemes

In this study, we examine the sensitivity of two contrasted cloud schemes. The first scheme is the prognostic cloud scheme developed by T93, and is used in the operational ECWFM forecasting system since April 1995. This scheme predicts the time evolution of two cloud variables: the fractional cloud cover a and the amount of cloud condensate l . T93 accounts explicitly for the physical sources and sinks leading to the production and dissipation of clouds. Clouds formed by convective processes are parameterized by considering them as condensates produced by cumulus updrafts and detrained in the environmental air. Clouds are also assumed to be formed by non-convective processes (e.g. large scale lifting of moist air, radiative cooling). Evaporation of clouds is described by two processes in connection with large-scale and cumulus induced subsidence and diabatic heating, and by turbulent mixing of cloud air with unsaturated environmental air. Precipitation processes are represented differently for pure ice clouds and mixed phase/pure water clouds.

2.1. Prognostic Cloud Scheme

The prognostic equations for l and a are written as:

$$\frac{\partial l}{\partial t} = S_{cv} + S_{bl} + C - E - G_p - \frac{1}{\rho} \frac{\partial}{\partial z} (\rho \overline{w'l'})_{entr} \quad (2.1a)$$

$$\frac{\partial a}{\partial t} = A(a) + S(a)_{cv} + S(a)_{bl} + S(a)_c - D(a) \quad (2.1b)$$

Sources of l and a are assumed to exist due to convection (S_{cv} and $S(a)_{cv}$), boundary layer turbulence at the top of mixed layers (S_{bl} and $S(a)_{bl}$) and due to non-convective condensation processes (C and $S(a)_c$). The decay of clouds occurs through evaporation for both variables (E and $D(a)$) and through the generation of precipitation (G_p) for cloud condensate only. The flux term on the right hand side describes the possibility of cloud destruction near cloud tops through cloud top entrainment for which no change of cloud fraction is assumed.

The various source and sink terms for the equation of cloud condensate are now described (their names as used in the computer code), since their sensitivity with respect to changes in temperature, specific humidity and vertical motion are examined in details in Section 4:

2.1.1. Convective clouds

$$LUDE = S_{cv1} = \frac{D_u}{\rho} l_u \quad (2.1.1a)$$

$$LDET = S_{cv2} = -\frac{D_u}{\rho} l \quad (2.1.1b)$$

where D_u is the detrainment of mass from convective updrafts, and l_u is the specific cloud water content in the updrafts.

$$LCUST = S_{cv3} = \frac{1}{\rho} M_c \frac{\partial l}{\partial z} \quad (2.1.1c)$$

where M_c is the cumulus-induced subsidence between the updrafts.

2.1.2. Stratocumulus clouds

$$LSCGE = S_{bl1} = -\frac{1}{\rho} \frac{\partial (\rho w^*)}{\partial z} (l_u - a l_d) \quad (2.1.2a)$$

where ρw^* is the cloud base mass flux evaluated from the moisture turbulent flux at cloud base and the vertical gradient of specific humidity in the boundary layer.

$$LFLEN = S_{bl2} = -\frac{1}{\rho} \frac{\partial}{\partial z} (\rho \overline{w'l'})_{entr} \quad (2.1.2b)$$

2.1.3. Cloud erosion

Cloud erosion due to turbulent mixing is described by:

$$L_{EROS} = E_2 = a K (q_s - q) \quad (2.1.3)$$

where K represents an inverse time scale.

2.1.4. Evaporation of clouds

$$L_{EVAP} = E_1 = a \frac{dq_s}{dt} ; \quad \frac{dq_s}{dt} > 0 \quad (2.1.4)$$

2.1.5. Stratiform clouds

$$L_{COND} = C = -a \frac{dq_s}{dt} ; \quad \frac{dq_s}{dt} < 0 \quad (2.1.5)$$

with

$$\frac{dq_s}{dt} = \left(\frac{dq_s}{dp} \right)_{ma} (\omega + g M_c) + \frac{dq_s}{dT} \left(\frac{dT}{dt} \right)_{diab}$$

where ω is the vertical velocity and M_c the convective mass flux. The vertical gradient of specific humidity at saturation is estimated along a moist adiabat (1st term). The actual computation of $\frac{dq_s}{dt}$ is done by first computing

$$T(t + \Delta t) = T(t) + \left(\frac{dT}{dp} \right)_{ma} (\omega + g M_c) + \left(\frac{dT}{dt} \right)_{diab},$$

$$\text{where } \left(\frac{dT}{dt} \right)_{diab} = \left(\frac{dT}{dt} \right)_{Dyn} + \left(\frac{dT}{dt} \right)_{LW} + \left(\frac{dT}{dt} \right)_{SW},$$

where r.h.s. terms stand for dynamical temperature tendencies, Long-Wave and Short-Wave temperature tendencies from radiative effects respectively. Finally, using the formula to compute saturation specific-humidity from temperature, we have

$$\frac{dq_s}{dt} \approx \frac{q_s(T(t + \Delta t)) - q_s(T(t))}{\Delta t}.$$

2.1.6. Precipitation processes

$$L_{PR} = G_p = \frac{1}{\rho} \frac{\partial}{\partial z} (\rho v_{ice} l_{ice}) + \frac{l}{c_0} \left[1 - \exp \left(- \frac{l}{a l_{crit}} \right)^2 \right] \quad (2.1.6)$$

The first term describes the ice sedimentation process with a falling speed v_{ice} (Heymfield and Donner, 1990) and the second term accounts for rain conversion in mixed phase and water clouds with two disposable parameters c_0 and l_{crit} (Sundqvist, 1978).

It is worth mentioning that the sequence of terms (2.1.1) to (2.1.6) above represents the actual sequence of computations in practice. Also, these processes are not totally independent of each other. More precisely, moist convection effects are first taken into account and these processes affect the environmental temperature

and saturation specific-humidity seen by the other processes. Those environmental T and q_s are not modified however by each of these terms following convection. All other terms are independent except for precipitation effects, where all previous terms affect LW/I and cloud fraction changes used in this computation.

2.2 Diagnostic Cloud Scheme

The second cloud scheme considered is a diagnostic scheme developed by Slingo (1987). It has the advantage of being simpler than T93 but it also describe physical processes more empirically and statistically. This scheme has been used operationally until the introduction of the prognostic scheme in 1995. A linearized (and adjoint) version is also currently being used in research mode at ECMWF in the context of 4D-Var assimilation where the scheme is coupled with long-wave and short-wave radiative effects. As in the prognostic scheme, three main cloud types are considered: convective clouds, stratiform clouds and stratocumulus.

Convective cloud cover is a function of the scale-averaged precipitation rate P produced by the moist convection scheme:

$$a_c = \alpha \log(P) + \beta \quad \text{with } a_c < 0.32 \quad (2.2.1)$$

It is worth mentioning that this precipitation rate P is taken as that at cloud base before any evaporation below the cloud and is averaged over a period of time. This latter averaging in time is not considered here. This total cloud cover is distributed along the vertical (between cloud base and cloud top) using a maximum overlap assumption.

Stratiform clouds are diagnosed as a function of relative humidity RH and of a critical relative humidity profile RH_c

$$a = \left[\frac{RH - a_c - RH_c}{1 - RH_c} \right]^2 \quad \text{with } 0 < a < 1 \quad (2.2.2)$$

Stratocumulus cloud cover is related to the strength of the inversion at the top of the boundary layer

$$a = \left[\gamma \left(\frac{\Delta\theta}{\Delta p} \right) + \delta \right] \left[1 - \mu (RH'_c - RH) \right] \quad (2.2.3)$$

where $\Delta\theta/\Delta p$ is the lapse rate of the most stable layer below 750 hPa and γ , δ and μ are empirical constants. The critical relative humidity RH'_c is set to 80 %.

Finally, cloud condensate l writes:

$$l = 10^{-4} a_c \quad \text{for convective clouds} \quad (2.2.4)$$

$$l = 0.05 q_s \quad \text{for other clouds} \quad (2.2.5)$$

The degree of empirism of this scheme for cloud condensate precludes any realistic description of rain formation.

3. Design of the experiments

This study is performed in a context relevant for operational data assimilation at ECMWF and also suits other currently operational environment at major centers. In order to cover a wide range of possible model states where the prognostic scheme is active in a regular time step of the forecast model, vertical profiles over six different areas over the globe are considered.

Zone	Convection type	Location
1	Deep convection in a mid-latitude frontal system	50/60 N – 320/330 E
2	Mid-level convection over continent	30/40 N – 110/120 E
3	Shallow cumulus convection in the tropics	20/30 N – 160/170 E
4	Deep convection along the ITCZ	0/10 S – 70/80 E
5	Stratocumulus regime in the sub-tropics	20/30 S – 270/280 E
6	Mid-level convection in a mid-latitude frontal system	50/60 S – 350/360 E

Table 1

The atmospheric profiles correspond to a 12-hour forecast from a T_L319L60 version of the ECMWF model (CY23R4) starting from the operational analysis at 12 UTC 15 January 2002. Since the ECMWF mass-flux scheme produces three main contrasted types of convection: deep, shallow and mid-level (hereafter referred to as type 1, 2, and 3 resp.), the cloud schemes are evaluated on atmospheric profiles associated with these three regimes. Figure 1a,b show the mean profiles of cloud condensate and cloud fraction produced by the prognostic scheme for the six zones.

4. Results

4.1. Jacobians for deep convective cases

Figure 2 shows the result of partitioning the contributions of the sensitivity (Jacobian) w.r.t T perturbations of the combined convection and cloud scheme operated in sequence (fractional stepping mode). These sensitivities were obtained for one deep convective point of region 1. This point exhibits typical properties encountered for all such convective regime of region 1. Other cases appear rarely where slightly different behavior occur. The first conclusion apparent in Fig. 2 is the dominance of four processes, i.e. detrained liquid water by convection, evaporation, cumulus-induced subsidence and finally precipitation effects (in order of importance). The dominant structures of the total jacobian is dominated by deep convective sensitivities. The scaling used in Fig. 2 is the same for all process shown. The low level sensitivity is the result of the strong sensitivity of moist-convection (detrainment term here) represented by Tiedtke's scheme, as already described in a previous study by Fillion and Mahfouf (2000). Perturbing temperature and especially moisture at the very lowest levels directly impacts the convective available potential energy (CAPE). This latter quantity is known to have a strong nonlinear dependance on these variables and is used as a crucial measure of convective intensity and closure assumption. It should be stressed that other convective schemes (e.g. Kain-Fritsch scheme) exhibits smaller sensitivity to those low-level perturbations even though CAPE is explicitly used. This comes from the mixture of the lifted parcel with the environmental air which tends to reduce the CAPE sensitivity as exemplified in Fillion and Belair (2002) with the Kain-Fritsch scheme. This mixture process is not performed in operational Tiedtke's scheme. The strong low-level sensitivity observed in Fig. 2 is thus strongly dependent on the assumptions made in the convective scheme.

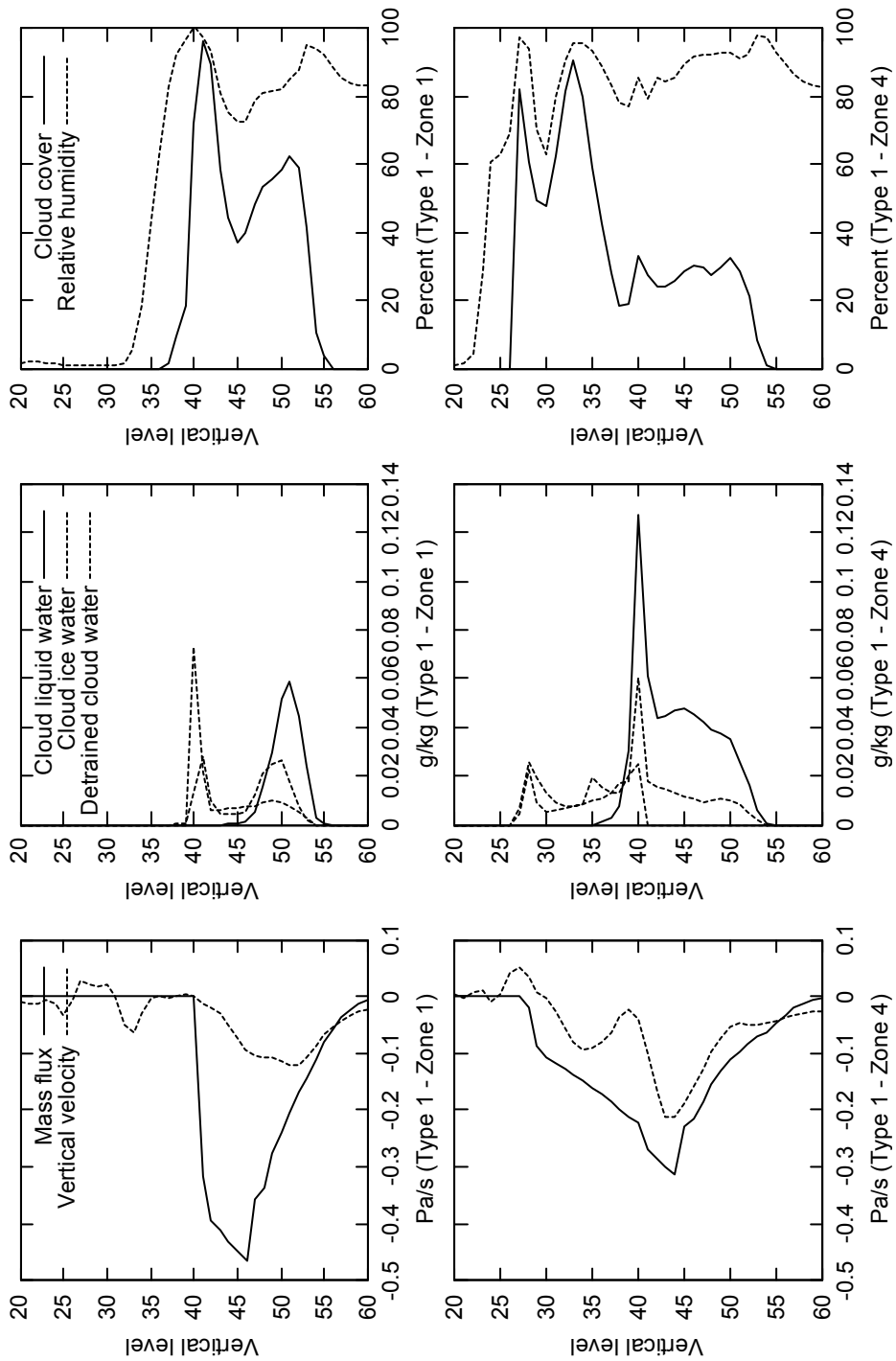


Figure 1a. Mean profiles of cloud condensate and cloud fraction produced by the prognostic scheme for the zones 1 and 4 of Table 1 (i.e. Deep Convection for a mid-latitude frontal system and along the ITCZ respectively).

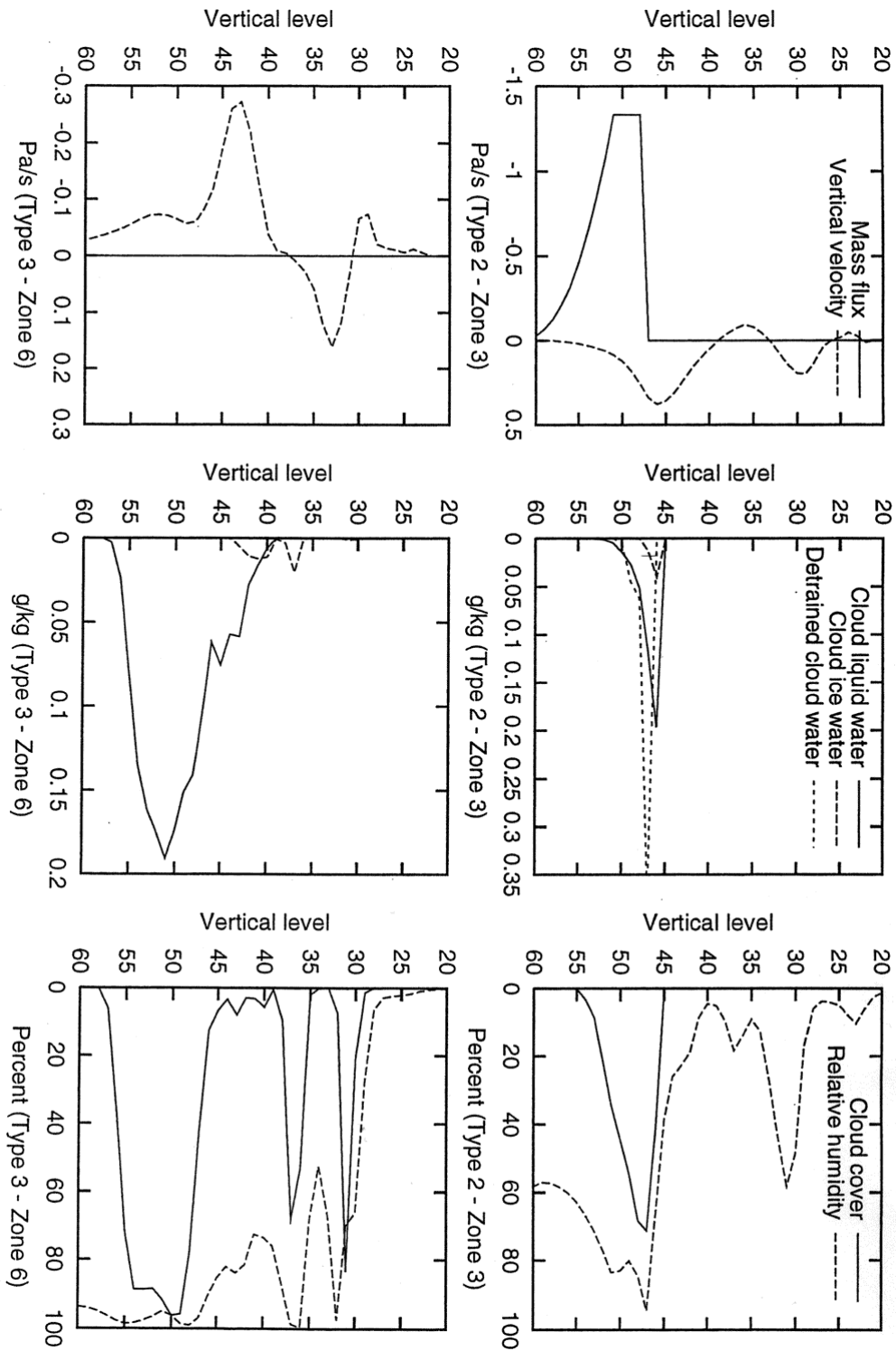


Figure 1b. Mean profiles of cloud condensate and cloud fraction produced by the prognostic scheme for the zones 3 and 6 of Table 1 (i.e. tropical shallow convection and mid-level convection for a mid-latitude frontal system).

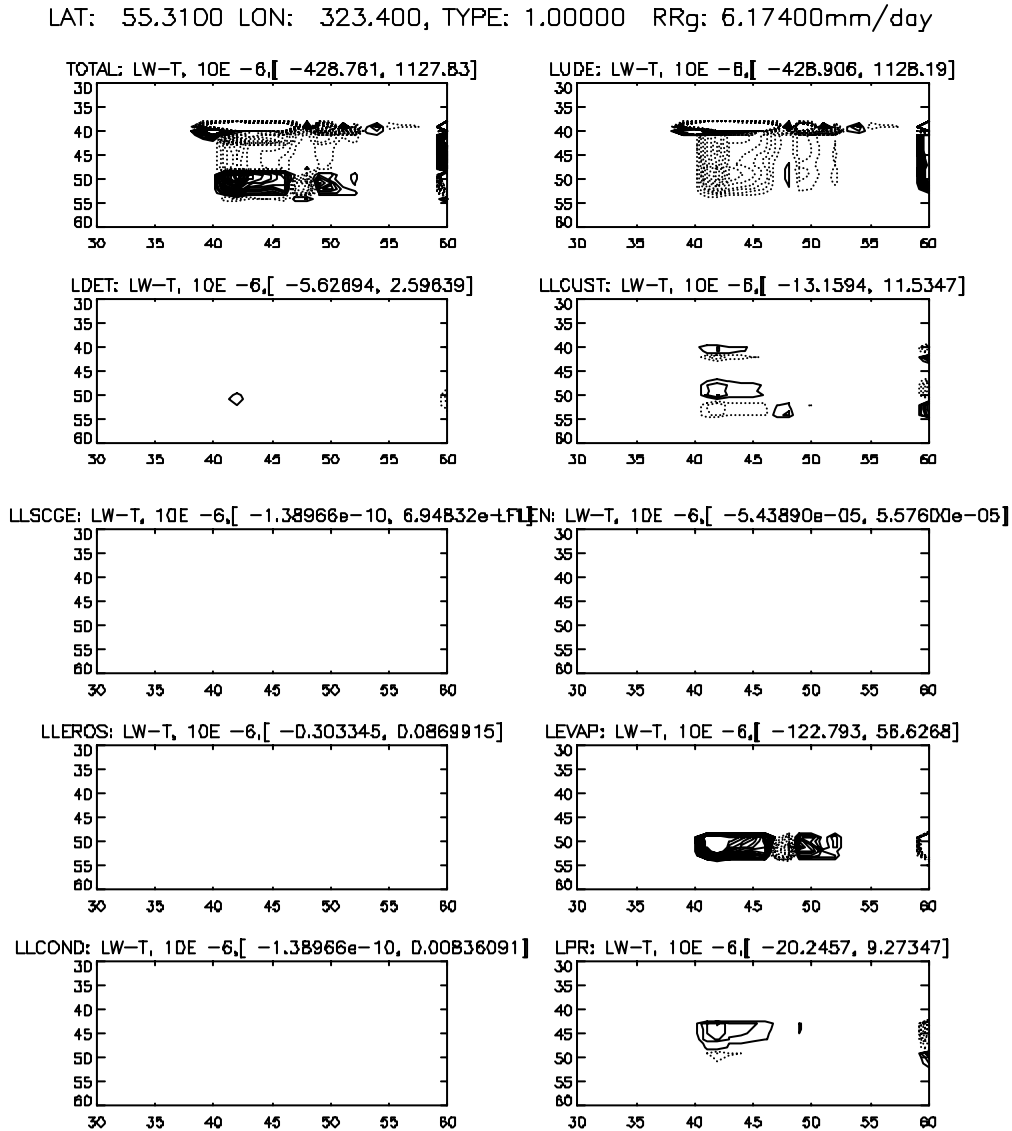


Fig. 2. LW/I jacobian w.r.t. temperature perturbations. Each contributing term of Eq. (2.1) are represented. [Min,Max] shown on top of each panels. Contouring is limited to fixed bounded contour intervals.

The positive and negative sensitivities observed in LUDE jacobian follows exactly the signs of the RR sensitivity (see Fig. 3). The sign structure in the LCUST jacobian follows exactly the sign of the vertical gradient of LW/I (ref. 2.1.1c) apparent in upper left panel of Fig. 6 (solid line). The LEVAP jacobian is the second most important contributor term and its lowest boundary is governed by cloud base and upper limit by the constraint that evaporation process cannot exceed available LW/I at that level. Here also, the sign structure follows exactly the RR or detrainment of LW/I sensitivity. Finally, the precipitation effects enters with about the least significant term in the total jacobian of LW/I, its structure being a complex mixture of all other previous terms (ref. Eq. 2.1.6).

LAT: 55.3100 LON: 323.400, TYPE: 1.00000, RRq: 6.17400mm/day

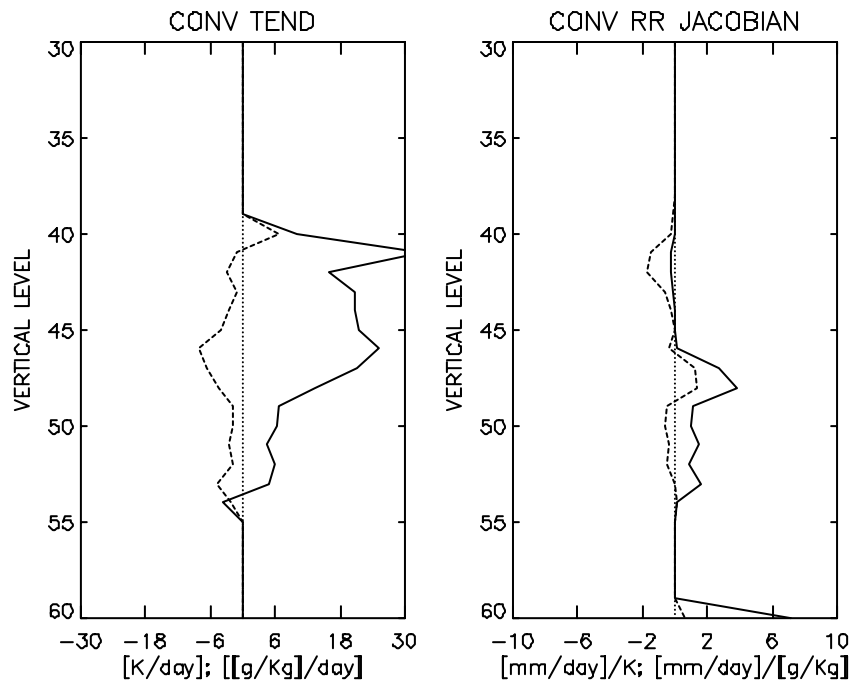


Fig. 3. Deep convective response and sensitivity for Tiedtke scheme. Upper left panel: Moistening-rate (solid) and heating-rate (dashed). Upper right panel: RR jacobian w.r.t. T (dashed) and q (g/Kg, solid).

Figure 4 shows the LW/I jacobian in terms of $\omega = \frac{dp}{dt}$, i.e. the environmental vertical velocity in pressure coordinates. Note that now, convection contributions are absent since Tiedtke's convective scheme only uses location of maximum vertical velocity as information from this field, so perturbing this field (assuming this does not change the location of the maximum at low level) does not change the result of moist-convection, then producing zero jacobian as seen in Fig. 4. For deep convective cases (type 1) the prognostic cloud scheme ignores totally by design any stratocumulus cloud effects (i.e. LLSCGE and LFLEN).

LAT: 55.3100 LON: 323.400, TYPE: 1.00000 RRg: 6.17400mm/day

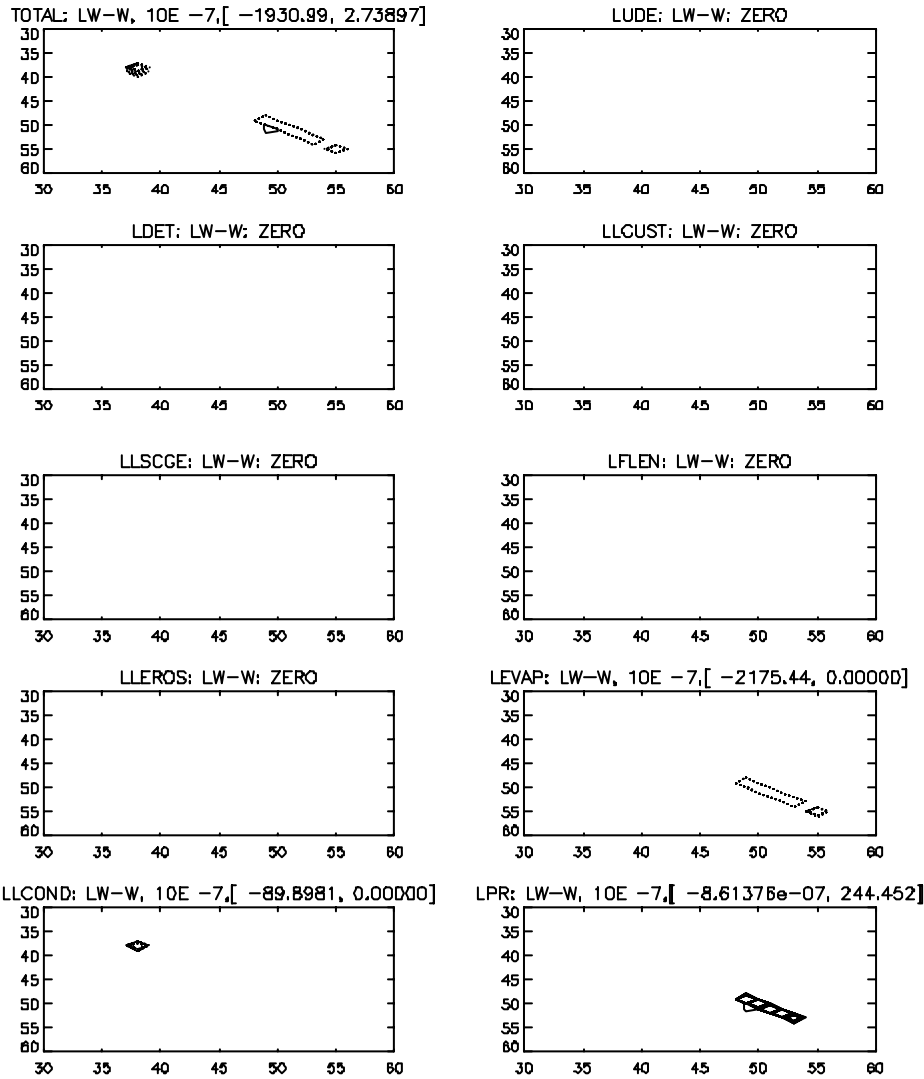


Fig. 4. Same as Fig. 2 but using perturbations on $w=dp/dt$ rather than T . Contouring limited to fixed bounded contour intervals.

The erosion of cloud effect is also unaffected by vertical velocity perturbations. The only contributors in such cases are thus just evaporation/condensation terms and precipitation effects. Those jacobians being quasi-diagonal. It is of interest to compare the significance of this sensitivity to vertical velocity perturbations as compared to T and q perturbations. We can write as a first approximation to liquid-water/ice perturbation

$$\delta LW = \frac{\partial LW}{\partial T} \delta T + \frac{\partial LW}{\partial q} \delta q + \frac{\partial LW}{\partial \omega} \delta \omega .$$

Assume we have in a vertical region of significant evaporation/condensation effects the following perturbation order of magnitudes:

$$\delta T = 1K \quad ; \quad \delta q = 0.1 \text{ g/Kg} \quad ; \quad \delta \omega = 0.01 \text{ Pa/s} .$$

Following the order of magnitudes of the respective jacobians shown in Fig. 2 and 4, we conclude that the sensitivity effects from vertical velocity perturbations are two to three orders of magnitude smaller than T

and q sensitivities. This relative importance of terms will be reexamined for shallow and mid-level convective regimes.

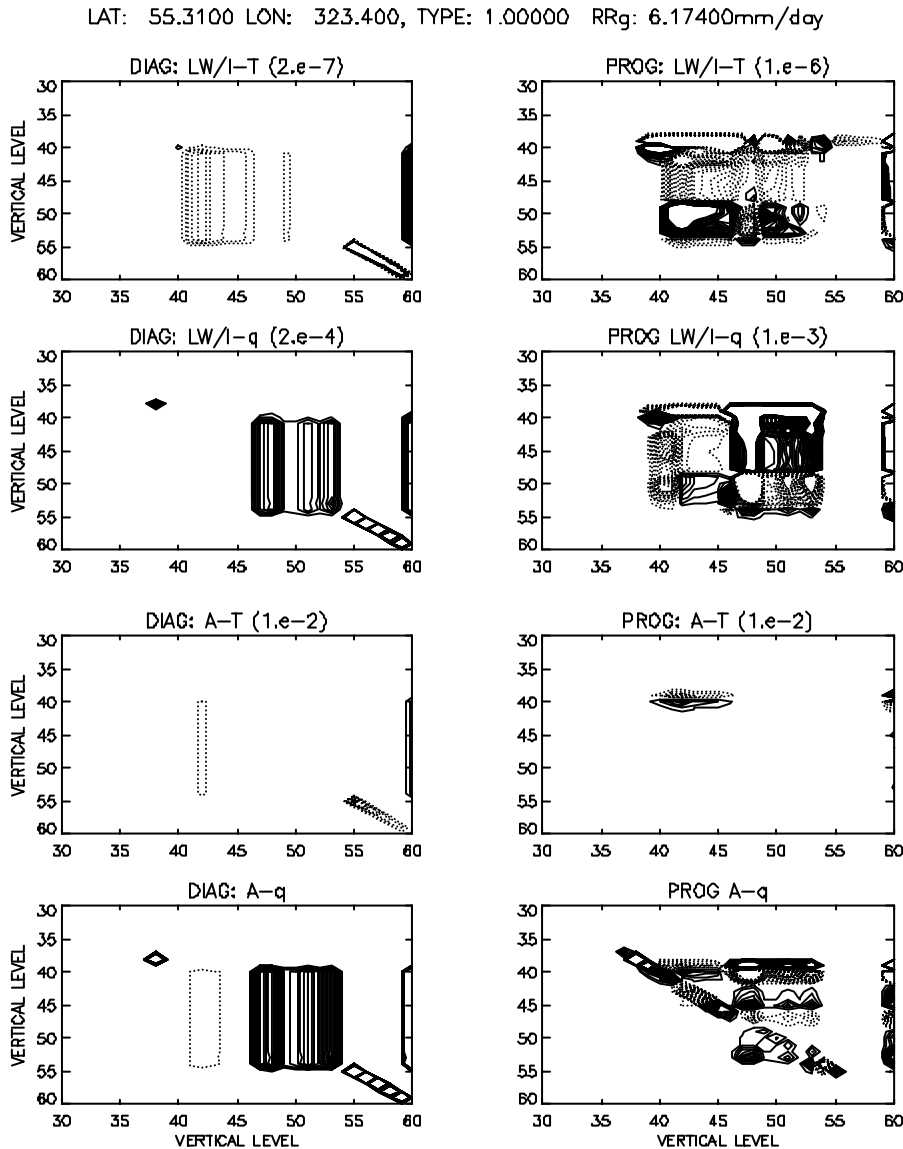


Fig. 5. Comparison of LW/I and Cloud fraction A jacobians w.r.t. T and q obtained with the Diagnostic scheme (left column) and prognostic scheme (right column). Contouring limited to fixed bounded contour intervals.

A comparison of sensitivities in terms of LW/I and cloud-fraction for diagnostic and prognostic schemes appear in figure 5. It is apparent that LW/I and cloud-fraction jacobians for the diagnostic scheme are strongly related and follows (2.2.4 and 2.2.1) for the convective contribution at least. Note that the diagnostic cloud scheme diagnoses cloud below the convective cloud base seen by the prognostic scheme (see also upper panels of Fig. 6). This is one obvious departure in terms of sensitivities apparent in Fig. 5 for both cloud schemes. The other obvious aspect is the amplitude and sign of the diagnostic jacobians driven by moist-convective effects. For instance, from cloud-fraction jacobian in terms of q perturbations (4th panel, left column), the negative and positive cells limitations follows exactly the signs of the RR jacobian in terms of q perturbations (see Fig. 3). Also, generally, the amplitude of diagnostic jacobians are smaller than prognostic jacobians. This relative amplitude between the two cloud schemes is also apparent for total (vertically integrated) LW/I (noted TLW) on Fig. 6 (lower panels) above the convective cloud base. It is

clearly obvious that both cloud schemes are largely driven by convection (through detrainment effects for the prognostic scheme and through the parameterization in terms of RR for the diagnostic scheme) in the convective cloud region. The amplitude of both TLM jacobians are different but their structure is identical in the convective cloud region. This has important implications for the assimilation of TLW satellite data with such cloud schemes in a variational context. Cloud sensitivities below convective cloud base is absent however for the prognostic cloud scheme.

All other deep convective point in zone 1 have similar properties as those discussed above.

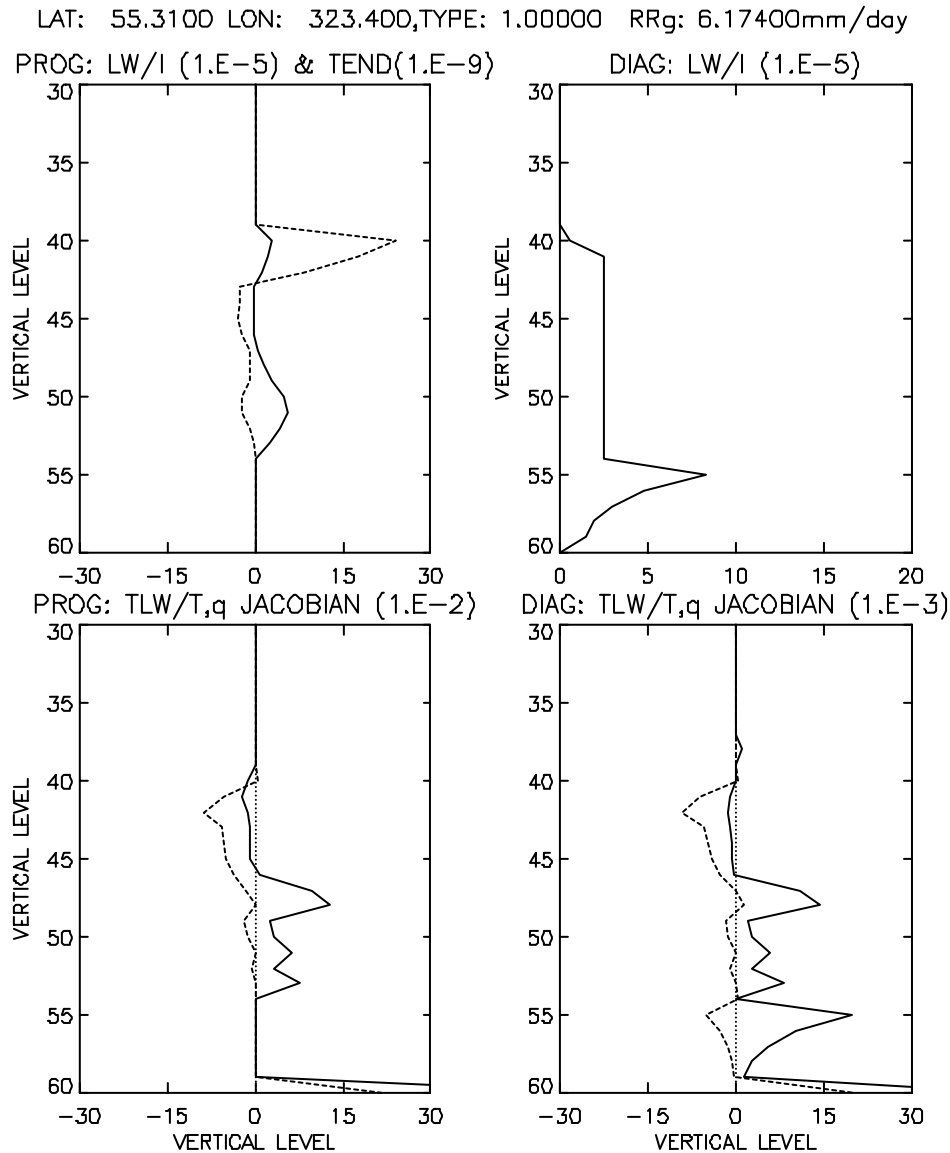


Fig. 6. Upper left panel: LW/I as computed with Tiedke prognostic scheme (solid line) and LW/I time-tendency (dashed line). Upper right panel: LW/I obtained from the Diagnostic scheme. Lower panels: Jacobians w.r.t. T (dashed line) and q (solid line) of the Total LW/I (TLW) for Prognostic and Diagnostic schemes.

4.2. Jacobians for shallow convective cases

We now show results in the case of shallow convection. A typical profile was chosen to represent zone 3 (tropics) and zone 5 (stratocumulus regime in the sub-tropics). Figure 7 shows the jacobian partitioning as in Fig. 2. Once again, jacobians from convective source terms are dominant, together with evaporation jacobian

but now the jacobian of erosion of clouds becomes important. This latter effect being mostly localized in the region of the convective response. Jacobians of LW/I in terms of q perturbations having similar structures as in Fig. 7 (results not shown). It is seen from Fig. 8 that the location of maximum intensity of sensitivity is more or less captured by the diagnostic scheme as compared to the prognostic cloud scheme. Non-diagonal structures appearing in the prognostic scheme being related to upper level detrainment (see Fig. 7, LUDE panel), are totally missed by the diagnostic scheme. Also, the diagonal part of the jacobian of cloud-fraction w.r.t. T is totally missed by the diagnostic scheme. Nevertheless, figure 9 lower panels show the comparison of TLW jacobians for the diagnostic and prognostic schemes. It is seen that for both T and q perturbations, the structure and location of maximum sensitivities are very similar for both schemes.

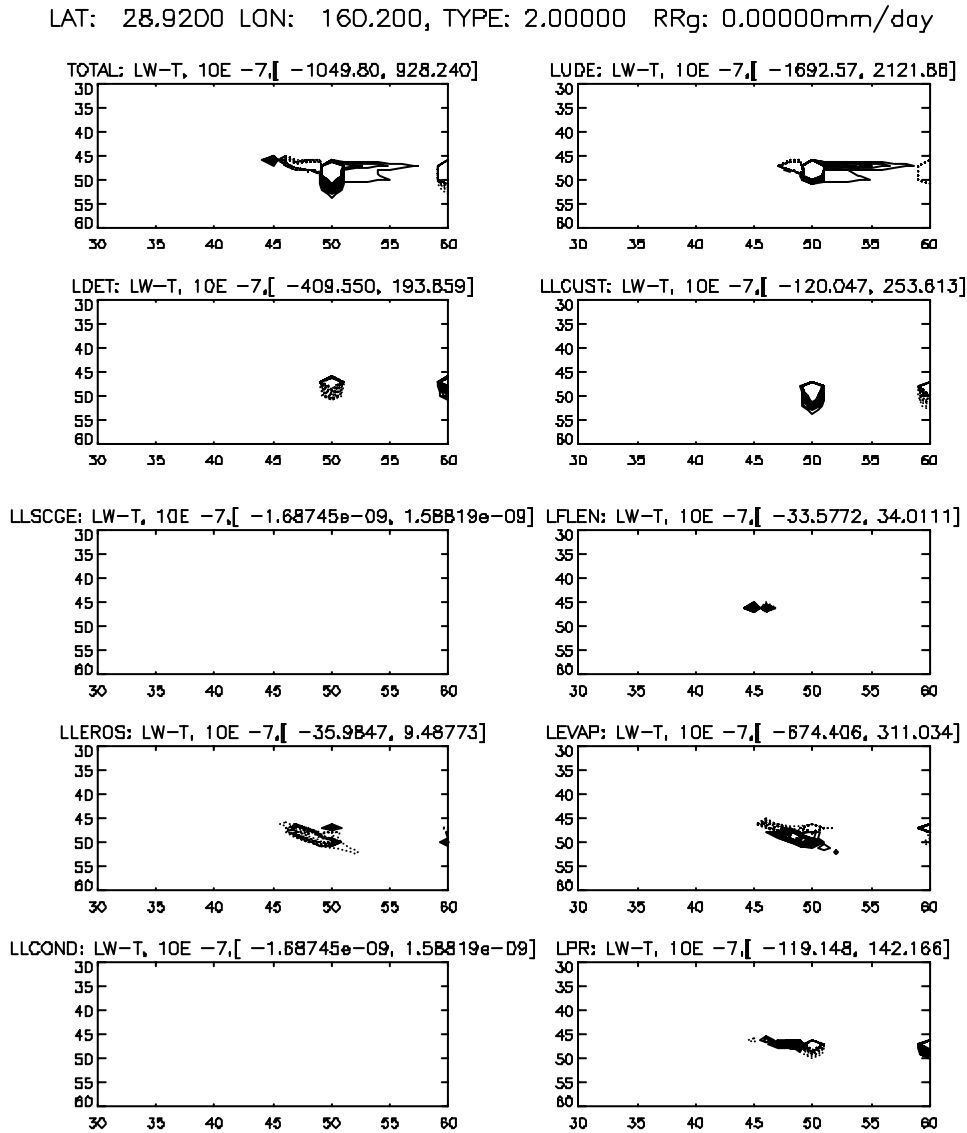


Fig. 7. Same as in Fig. 2 but for shallow convection type of zone 3.

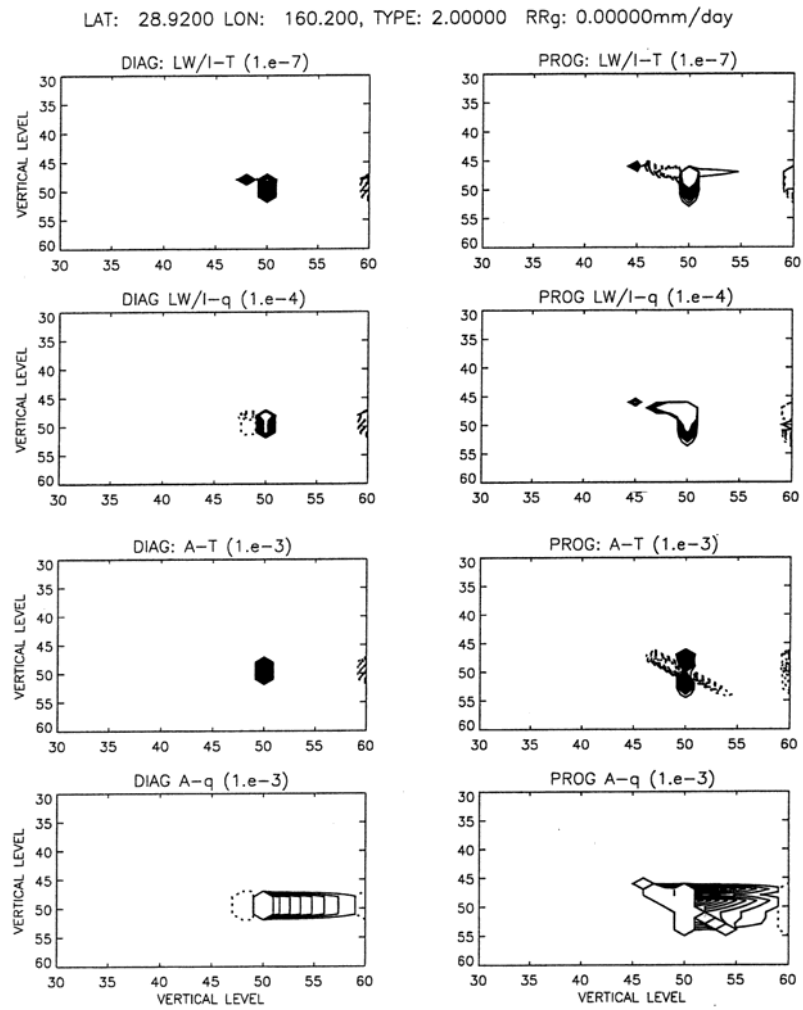


Fig 8. As in Fig. 4 but for a point in zone 6 representative of mid-level convection regime.

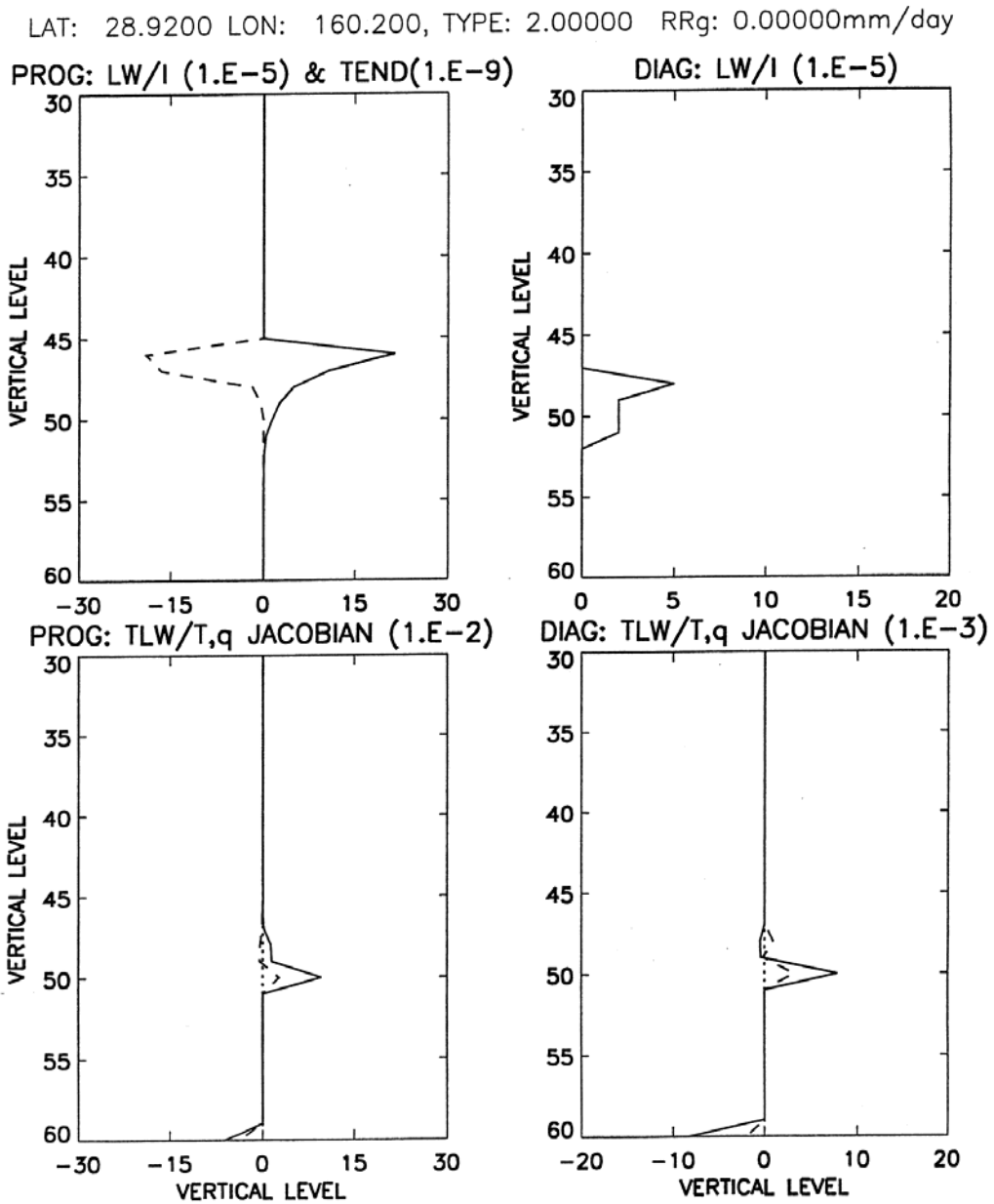


Fig. 9. As in Fig. 6 but for a point in zone 3 representative of shallow convection regime.

LAT: -55.3100 LON: 359.100, TYPE: 3.00000 RRq: 0.00000mm/day

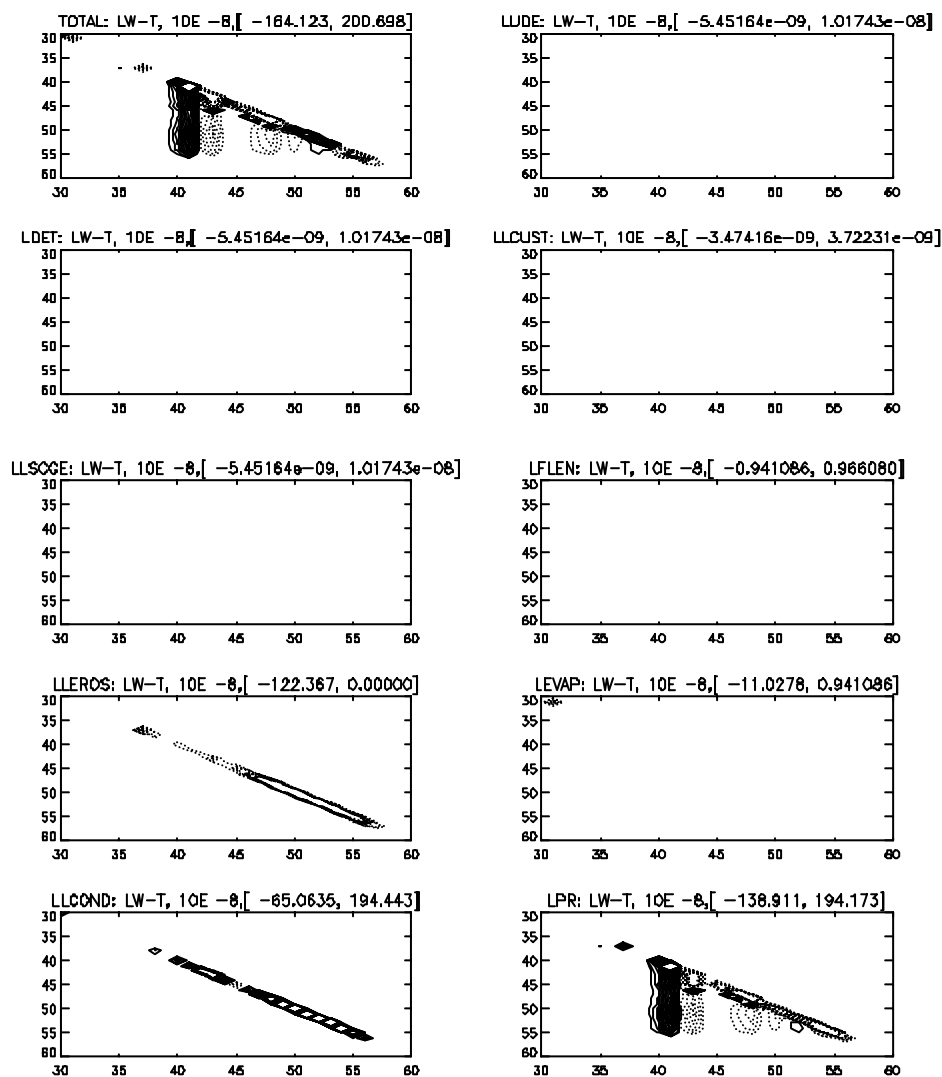


Fig. 10. As in Fig. 2 but for a point in zone 6 representative of mid-level convection regime.

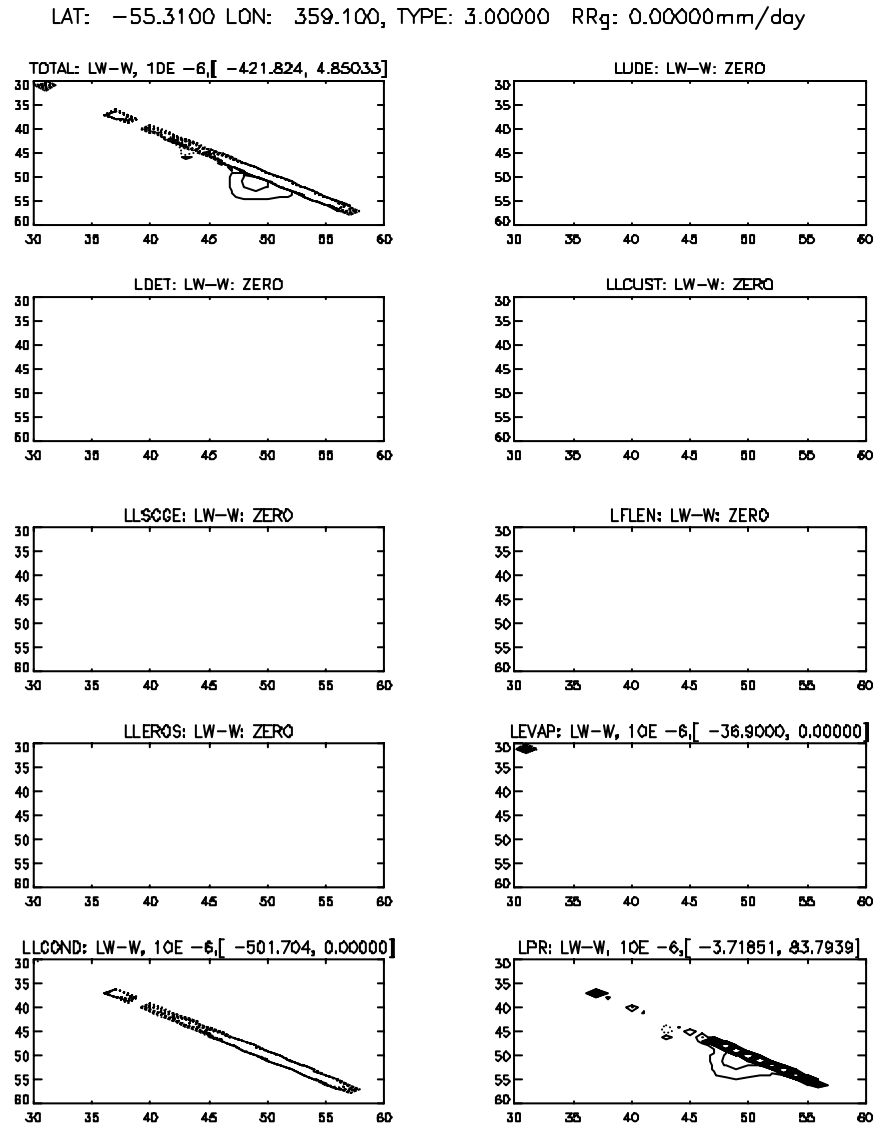


Fig. 11. Same as in Fig. 4 but for a point of zone 6 representative of mid-level convection.

4.3. Jacobians for mid-level convective cases

This type of convective regime is localized over a generally thin vertical domain with weak convective detrainment (ref. Figs. 1a,b). As opposed to the previous two other types of convective regime, the prognostic cloud scheme in such cases is less dominated by convection effects. Figure 10 shows LW/Iacobians w.r.t. T perturbations. It is seen that the jacobian from erosion, condensation and precipitation effects dominate. Other terms being extremely weak. Erosion and condensation jacobians have diagonal structures basically because of the simple form of dependency of these effects in terms of temperature (ref. Eq. 2.1.3 and 2.1.5) and the fact that moist convection does not act to distort the temperature field used as input to the cloud scheme as in other cases examined in sub-section 4a,b. Jacobians in terms of q perturbations have similar structures (results not shown). It is interesting to compare the TLW/Iacobians in terms of vertical velocity perturbations (Figure 11) and those of T (or q) perturbations. Condensation and precipitation jacobians now dominate. The former jacobian still being diagonal again because of the simple dependency of this term to vertical velocity field (ref. Eq. 2.1.5) and absence of moist-convection effects. An important aspect to notice is that, under the same orders of magnitude estimate of T, q and vertical velocity perturbations as done

above, the jacobians of TLW/I w.r.t vertical velocity becomes as important as jacobians in terms of T or q. This was not the case for previous results for deep and shallow convection regimes.

5. Summary and conclusions

In this study, sensitivities of ECMWF prognostic and diagnostic cloud schemes have been examined. This was done for a wide range of convective regimes over the globe. Jacobians of LW/I and cloud fraction were computed by coupling (as in the forecast model) Tiedtke's convective scheme with cloud scheme. The atmospheric profiles considered correspond to a 12-hour forecast from a T₁319L60 version of the ECMWF model (CY23R4) starting from the operational analysis at 12 UTC 15 January 2002. Since the ECMWF mass-flux scheme produces three main contrasted types of convection: deep, shallow and mid-level (hereafter referred to as type 1, 2, and 3 resp.), the cloud schemes are evaluated on atmospheric profiles associated with these three regimes.

Results obtained demonstrate the strong dependence of LW/I jacobians (T and q perturbations) to moist-convective terms in the cloud scheme. Evaporation/condensation effects are also important for such convective regimes together with precipitation effects (least important). In particular, a very strong sensitivity of TLW/I was observed at upper levels because of the strong detrainment sensitivity by convection at these upper levels, which directly impact cloud sensitivities. The jacobians in terms of vertical velocity perturbations is negligible as compared to T or q perturbations for such convective cases. For shallow convection regime, source terms from convection still dominate together with evaporation effects but now erosion becomes important (although least important). Because of the dominance of the convection terms on cloud sensitivities for deep and shallow convection, it was found that the total LW/I (TLW) jacobian for such convective regimes for the prognostic scheme was well approximated by the jacobian using the diagnostic scheme between convective cloud base and top. The amplitude of the two however were different (diagnostic TLW weaker). This shows that for such convective regimes, assimilation of satellite data related to such quantities can be envisaged with a tangent-linear (TL) and adjoint (ADJ) code of a diagnostic cloud scheme. This fact simplifies the definition of the control variables of the minimization, although when such cases occur, the TL and ADJ of the prognostic cloud scheme being very simple to construct using source terms from convection mostly. It was also found that for mid-level convection regimes, jacobians of LW/I and cloud fraction in terms of vertical velocity perturbations were as important as jacobians w.r.t. T and q perturbations. The structure of these jacobians being essentially diagonal for those perturbations because of the weak effects from convection and the functional dependence of the dominant jacobian terms (condensation, erosion) w.r.t these perturbations. Non-diagonal jacobian structures were found for deep and mid-level convective regimes (not present for shallow-convection cases), this being the result of a complicated form of this process in terms of all other processes entering the prognostic cloud scheme.

A necessary continuation of this work should involve a careful examination of cloud conditional occurrence for a wide range of convective regimes and quantification of the degree of nonlinearity of the prognostic cloud scheme. These additional results in combination with those presented here could clarify the potential use of these ECMWF cloud schemes for the assimilation of satellite data over cloudy regions.

Acknowledgments: The authors would like to acknowledge stimulating discussions with researchers of the data assimilation group at ECMWF during a one month visit of the first author at ECMWF.

References

- Fillion, L. and S. Belair, 2002: Tangent-Linear and Adjoint of the Kain-Fritsch Moist-Convective parameterization. To be submitted to *Mon. Wea. Rev.* Sept. 2002.
- Gregory, D., J.-J. Morcrette, C. Jakob, A.C.M. Beljaars, and T. Stockdale, 2000: Revision of convection, radiation and cloud schemes in the ECMWF Integrated Forecasting System. *Quart. J. Roy. Met. Soc.*, **126**, 1685-1710
- Heymsfield, A.J and L.J. Donner, 1990: A scheme for parameterizing ice-cloud water content in general circulation models. *J. Atmos. Sci.*, **47**, 1865-1877
- Janiskova, M., J.F. Mahfouf, F. Chevallier, and J.J. Morcrette, 2000: Linearized physics for the assimilation of cloud properties. ECMWF/Euro TRMM Workshop on Assimilation of clouds and precipitation. 6-9 Nov, 2000.
- Sundqvist, H., 1978: A parameterization scheme for non-convective condensation including prediction of cloud water content. *Quart. J. Roy. Met. Soc.*, **104**, 677-690
- Tiedtke, M., 1989: A comprehensive mass flux scheme for cumulus parameterization in large scale models. *Mon. Wea. Rev.* **117**, pp 1779-1800.
- _____, 1993: Representation of clouds in large-scale models. *Mon. Wea. Rev.* **121**, pp 3040-3061.
- Slingo, J.M., 1987: The development and verification of a cloud prediction scheme for the ECMWF model. *Q. J.R. Meteorol. Soc.*, **113**, pp 899-927.
- Thompkins, A., 2002. A prognostic parameterization for subgrid-scale variability of water-vapor and clouds in large-scale models and its use to diagnose cloud cover. *J. Atmos. Sci.*, **59**, 1917-1942.